Rock Mechanics Bulletin 5 (2026) 100278

Contents lists available at ScienceDirect

Rock Mechanics Bulletin

journal homepage: www.keaipublishing.com/en/journals/rock-mechanics-bulletin

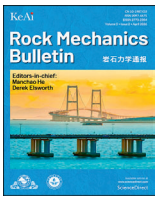

From lab forces to field lifespans: How rock and operating parameters govern TBM disc cutter wear

Ehsan Mohtarami[a,*], Amin Hekmatnejad[b], Georg H. Erharter[c], Alvaro Pena[d]

[a] Department of Civil and Geomechanics Engineering, Arak University of Technology, Arak, Iran
[b] Departamento de Ingeniería de Minería, Escuela de Ingeniería, Pontificia Universidad Cat'olica de Chile, Chile
[c] Norwegian Geotechnical Institute, Sandakerveien 140, Oslo, Norway
[d] Escuela de Ingeniería de Construcci'on y Transporte, Pontificia Universidad Catolica de Valparaíso, Chile

ARTICLE INFO

Keywords:
Rock cutting
Tunnel boring machine
Explicit finite element method
Wear
Cutter lifespan estimation

ABSTRACT

Tunnel boring machines (TBMs) are considered a reliable and fast method for boring long tunnels. However, the wear and failure of disc cutters in hard rock influences the efficiency of equipment, ultimate timeline, and project cost. Therefore, estimating the cutter life under different geomechanical conditions is crucial for TBM manufacturers and tunnel engineers. This study investigates the influence of geomechanical factors, including elastic modulus (E), uniaxial compressive strength (σ_c), confining stresses, and TBM operational parameters such as penetration rate (P) and disc cutter inclination angle (ϕ), on disc cutter wear using the explicit finite element method. The results revealed that the uniaxial compressive strength, disc cutter inclination angle, rock elastic modulus, and confining stresses, in that order, had the greatest impact on the cutter wear rate. Such that an increase in compressive strength from 31 MPa to 137.9 MPa caused a 2.4-fold reduction in cutter life. Meanwhile, the cutter life in the rock without confining stress was only 15% greater than in the sample under 15 MPa of confining stress. Additionally, to achieve the most optimal and economical drilling conditions, the penetration depth of the disc cutters should be optimized based on the existing conditions. Since the installation location of the disc cutters, their spacing and rotational trajectory significantly influence wear levels, a full-scale simulation of a TBM is conducted according to a real case study. The comparison of results indicated that the proposed method has high capability in estimating the cutter life under various geomechanical conditions.

1. Introduction

Tunnel boring machines (TBMs) were created in the early 19th century as a result of the rapid growth in technology for underground space excavation. Despite the high initial investment, the speed and high-quality drilling capability of these machines have made them competitive with traditional excavation methods for long tunnels. However, the efficiency of mechanized drilling in hard rocks is directly influenced by the performance of the cutting tools. Cutting forces are the main factor governing cutting efficiency (Cho et al., 2010). However, these forces also directly act on the disc cutters, causing wear. Progressive disc cutter wear successively decreases cutting efficiency until an effective excavation process is not possible anymore. Replacing worn disc cutters can significantly impact the final time and cost of a tunneling project by reducing the gross advance rate. Statistically, disc cutter failure costs account for at least one-fifth of the project expenditures, which can rise to one-third in extremely hard rocks (Wan et al., 2002). The time spent replacing disc cutters has also been noted to account for nearly one-third of the overall project duration (Su et al., 2010). Estimating the advance rate and efficiency of TBMs has attracted significant attention from researchers (Jing et al., 2021; She et al., 2024). However, without considering disc cutter wear in these estimates, the accuracy will be insufficient.

Various approaches (including full-scale (Gertsch et al., 2007; Thyagarajan and Rostami, 2024) and small-scale (Espallargas et al., 2015; Macias et al., 2016) laboratory cutting tests, theoretical (Oggeri and Oreste, 2012; Zhang et al., 2019) or empirical models (Hassanpour et al., 2014, 2015; Liu et al., 2017), and numerical methods (Cho et al., 2010; Li and Du, 2016; Yang et al., 2016)) have been employed to understand the rock fragmentation mechanism by disc cutters and the wear

* Corresponding author.
E-mail address: e.mohtarami@arakut.ac.ir (E. Mohtarami).
Peer review under the responsibility of Chinese Society for Rock Mechanics & Engineering.

https://doi.org/10.1016/j.rockmb.2025.100278
Received 28 July 2025; Received in revised form 20 October 2025; Accepted 29 November 2025
Available online 2 December 2025

of drilling tools. In the field of theoretical research, due to the complex nature of the subject, relatively fewer studies are available. For example, Roxborough and Phillips (1975) theoretically investigated the vertical and rolling forces acting on the disc as a function of penetration depth, disc cutter tip angle, and uniaxial compressive strength of the rock. Later, researchers used these relationships to calculate the amount of wear (Agrawal et al., 2021; Yang et al., 2021). Wang et al. (2012) examined TBM performance parameters related to disc cutter wear, analyzed the applied forces, and proposed an energy-based law for disc cutter wear estimation. Oggeri and Oreste (2012) predicted TBM advance rate by incorporating the cutter life index (CLI) and disc cutter wear into Barton's classification system calculations. However, analytical solutions are applicable for relatively simple conditions and limited input parameters.

Most laboratory studies pertain to studying the rock cutting mechanism using the linear cutting machine (LCM). For example, Chang et al. (2006) used the LCM to determine optimal cutting conditions for Hwangdeung granite and examined normal and rolling forces as functions of penetration depth and cutter spacing. Zhao et al. (2015), by repeating the LCM test for vertical and inclined disc cutters, found that due to the disc cutter inclination and different cutting forces, the rock-damaged area was completely different in these two scenarios. Ma et al. (2016) investigated the influence of confining stresses on the forces applied to the disc cutter using full-scale cutting tests on granite samples, noting that confining stresses significantly influence normal and rolling forces. Lin et al. (2017) conducted laboratory-scale cutting tests using several disc cutters and different rock types, stating that disc cutters should be designed and manufactured according to geological conditions to minimize wear. Sun et al. (2019) used 1:10 scale laboratory tests to propose a model for estimating disc cutter wear and rock abrasiveness. Although full-scale tests offer significant advantages, they are expensive and time-consuming.

In the field of actual field data, Hassanpour et al. (2014, 2015) analyzed disc cutter wear data from various tunneling projects in Iran, providing a relationship between wear and intact rock parameters (such as uniaxial compressive strength and rock Vickers hardness number) and rock mass parameters (such as RQD and basic RMR). Liu et al. (2017) studied the wear of 20-inch constant cross-section (CCS) disc cutters, developing a model to estimate their wear in rock based on the Cerchar Abrasivity Index (CAI) and UCS. The most common models for estimating wear rates are those developed by the Colorado School of Mines (CSM) (Rostami, 1997), NTNU (Bruland, 2000), and Gehring (1995). The CSM model uses CAI to determine the basic cutter life and provides an estimate of the number of disc cutters required, time, and costs (Rostami, 1997). While, the NTNU model estimate considers rock abrasiveness based on a specific parameter called the Cutter Life Index (CLI) (Bruland, 2000). The Gehring model uses data from various projects to plot the relationship between CAI and the weight loss of disc cutters due to wear (Gehring, 1995). Some studies have also linked wear with rock mass classification (Wang et al., 2020). However, according to research by Schneider et al. (2012), these methods often yield highly variable results. Additionally, due to rapid advancements in disc cutter manufacturing technology, wear estimation models need to be updated with newer data (Bruland, 2000). The accuracy and reliability of these models depend on the quality and quantity of available data (Xiao et al., 2017). On the other hand, the main shortcoming of these methods is associating wear with a single or two rock abrasive or strength parameters (Hassanpour et al., 2014; Liu et al., 2017) where high correlation coefficients are often not observed.

The shortcomings of empirical models and the high time and financial costs of laboratory tests on the one hand and the development of numerical models on the other have encouraged researchers to use numerical methods to study the rock cutting mechanism by disc cutters. Among these, the finite difference method (FDM), discrete element method (DEM), and finite element method (FEM) have garnered more attention. Innaurato et al. (2007) generalized a two-dimensional model utilizing FLAC software to study the effect of confining stress and cutter spacing on rock fracture and chipping formation, using the Mohr-Coulomb constitutive model. Gong et al. (2006a), Gong and Zhao (2009), Gong et al. (2005, 2006b) examined the influence of joint spacing and orientation on rock fragmentation using UDEC software in 2D. They indicated that the orientation and spacing of the joints can significantly affect crack initiation, propagation, as well as fragmentation patterns. Moon and Oh (2012) used PFC software to predict disc cutter forces in cutting tests and understand the damage zone. Cho et al. (2010) used AUTODYN to simulate linear cutting tests and investigate the effect of cutter spacing on the applied forces. Li and Du (2016) employed an extended Johnson-Cook and Drucker-Prager damage model to simulate rock fragmentation due to TBM disc cutters by considering the role of strain rate. Recently, researchers have utilized the peridynamics method in rock fragmentation phenomena, overcoming the weaknesses of FEM and DEM in simulating rock cutting in mixed grounds (Shang et al., 2023, 2024, 2025; Zhou et al., 2018). Despite numerical studies on rock-cutter interaction, limited reports on disc cutter wear laws are available. The lack of such studies can be attributed to the sensitive nature of data that TBM companies and tunnel constructors handle, limiting researchers' access to disc cutter wear data (Schneider et al., 2012). In this regard, Jian et al. (2015) compared stresses under a single disc cutter in hypothetical worn and unworn conditions, their study did not propose a method for measuring wear, though. Yang et al. (2016) by developing the theoretical model of Li et al. (2011) which was presented for wear, proposed a new wear model with vertical and rolling forces as the primary inputs. Later, Zahiri et al. (2020) developed their method by considering variable wear on the disc cutter body.

However, the study of cutter wear phenomena still requires further investigation. Moreover, a comprehensive study on the effect of various geomechanical parameters on disc cutter wear is not available. Therefore, this research aims to investigate the impact of varying parameters such as elastic modulus (E), uniaxial compressive strength (σ_c), penetration rate (p), confining stresses, and disc cutter inclination angle (ϕ) on wear using the explicit finite element method (LS-DYNA). It should be mentioned that the role of the disc cutter inclination angle and the rock's elastic modulus on tool wear has not been addressed so far. So, after the introduction, the governing equations of the wear phenomenon will be explained (Section 2). Then, the numerical modeling conditions will be presented and supported by comparing the results with LCM test results (Section 3). In Section 4, the effect of geomechanical parameters on tool wear is investigated. It is noteworthy that in a real case, during the construction of the Gelas water conveyance tunnel in northwest Iran, a specialized database was compiled, encompassing real disc cutter wear and geological data from different tunnel layers, which was subsequently analyzed. To further strengthen the proposed method, the full cross-section tunnel excavation process is simulated, and numerical wear results are compared with real data, with interpretations provided in Section 5. The results are discussed in Section 6 and finally, conclusions are presented in Section 7.

2. Numerical simulation methodology (theory and modeling)

2.1. Governing laws of the wear problem

In contact mechanics theory, two types of motion are possible in the contact between two bodies: sliding (displacement of the contact point between two surfaces) and rolling (relative motion of the two surfaces along the contact plane) (Johnson, 1985). In the contact between rock and disc cutter, both rolling and sliding transpire concurrently, due to the curved path and existing friction. The slip ratio for rolling objects is defined as the ratio of the sliding interval to the overall rolling interval (Goryacheva and Goryachev, 2006; Li et al., 2011; Yang et al., 2016). Consequently, the sliding speed (V_s) can be determined using contact theory in the following manner (Johnson, 1985; Li et al., 2011),

$$V_s = \eta\, V_t \tag{1}$$

where the slip ratio, denoted as η, and V_t is the disc cutter's tangential speed, which are calculated as Eqs. (1) and (2),

$$\eta = \frac{\mu\, b}{R_w}\left[1 - \sqrt{1 - \frac{F_{rs}}{\mu\, F_n}}\right] \tag{2}$$

$$V_t = 2\pi R_i \omega_r \tag{3}$$

where, F_n is the normal force applied to the disc cutter, and F_{rs} is the resultant of the rolling force F_r and the lateral force F_s (Fig. 1a). If the lateral forces acting on the disc cutter cancel each other out (e.g., in the LCM test), this force is equal to the rolling force F_r. The contact area width is denoted by b, μ is the dynamic coefficient of friction between the rock and the disc cutter (for more details, readers can refer to (Erharter et al., 2023)), R_i is the installation radius of the disc cutter, which is the distance between the center of the cutterhead and the disc location, ω_r is the cutter head rotational speed in revolutions per minute, and R_w is the instantaneous radius of the disc cutter, in other words, it can be calculated from the difference between the radius of the intact disc cutter and the amount of wear.

In the previous experimental research made to measure the wear, a sliding tribometer with crossed cylinder contact is used (Huq and Celis, 2002; Ramalho and Miranda, 2006). In this apparatus, a cylinder of the desired metal sample (part 1 in Fig. 1b) is brought into contact with a reference sample that has specific mechanical properties (part 2 in Fig. 1b). These two samples are pressed together using a force application system (part 3 in Fig. 1b), while the applied force and energy are recorded by a data logger (part 4 in Fig. 1b). Finally, by measuring the volumetric wear and plotting it against the consumed energy, their relationship is determined. Thus, the wear rate energy is defined as the ratio of the disc cutter's abrasive volume to the frictional power (Li et al., 2011). One may represent the volumetric wear (or bulk wear) of the disc cutter W_V during the tunneling operation as follows,

$$W_V = C_H\, I\, M \tag{4}$$

where, in the specified experimental conditions, I represents the wear energy, which is the disc cutter's bulk wear per unit of frictional power. C_H is a coefficient that is contingent upon the hardness and material type and is inversely related to hardness (Ramalho and Miranda, 2006). If the material of the disc cutter ring is entirely uniform, this coefficient equals 1. Zahiri et al. (2020), using a laboratory approach in accordance with ASTM standards (ASTM E92 and ASTM E384-16), demonstrated that the hardness of the disc cutter decreases from its edge towards the core. Considering the reduction of wear resistance when the material hardness decreases, the coefficient C_H varies inversely with the hardness of the disc cutter. In other words, under completely identical conditions, as the disc cutter wears from the edge toward the core, the amount of volumetric wear increases. Therefore, manufacturing companies have tried to reduce this effect by widening the cutter geometry in the CCS type, which will be discussed in the following sections. To determine the C_H coefficient experimentally in the laboratory, the disc cutter is sectioned at several points and subjected to hardness measurement tests. Finally, the hardness values at all points of the disc cutter, from the surface to the core, are interpolated using the obtained data. The C_H coefficient is 1 at the surface and is calculated at any point as the ratio of the surface hardness number to the hardness number at the point in question. For the present study, hardness tests were conducted, and the C_H coefficient varies linearly from 1 at the surface to 1.4 at the depth. M also represents the frictional power in Eq. (4). The friction law states that the product of sliding distance and frictional force is sliding frictional power. Therefore, the following is an expression for the frictional power,

$$M = \mu\, F_n\, V_s\, t \tag{5}$$

where t is the boring time, which can be determined in the following manner,

$$t = D/V_{tb},\, V_{tb} = p_{rev}\cdot\omega_r,\, p_{rev} = P\cdot N \tag{6}$$

where P is the penetration depth, D is the boring distance, V_{tb} is the overall tunnel boring velocity of the cutterhead, p_{rev} is the penetration depth of the cutterhead per revolution, and N is the number of disc cutters used on the cutterhead at the specified distance of R_i. It is noteworthy that for a given rock mass and a specific material of the disc cutter, μ and I can be measured. With the help of the aforementioned equations and by elaborating on Eq. (4), the volumetric wear can finally be calculated,

$$W_V = 2\pi\, C_H\, I\, \mu^2\, F_n\, R_i\, D\cdot\cos^{-1}\left(\frac{R_w - P}{R_w}\right)\cdot\left[1 - \left(1 - \frac{F_{rs}}{\mu\, F_n}\right)^{1/2}\right] \Big/ (P\cdot N) \tag{7}$$

By determining F_n and F_{rs}, the amount of wear can be calculated. However, as the disc cutter wears, the normal and rolling forces applied to the cutter, the radius of the worn disc cutter (R_w), and the abrasive hardness coefficient (C_H) will also change, leading to a variable wear rate. This means that the wear rate of the cutter is not constant and changes with the geometry of the disc cutter. This highlights the importance of updating the disc cutter's geometry during rock cutting to accurately calculate the amount of wear-a factor that has received little attention.

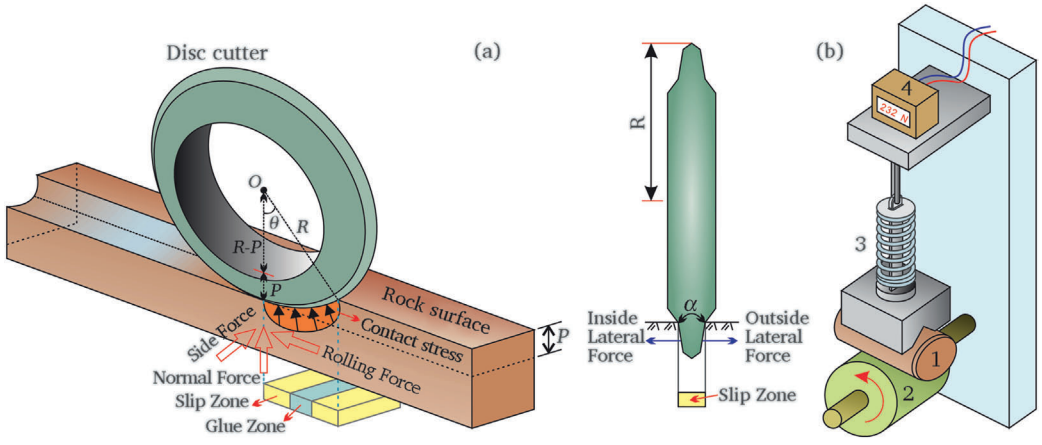

Fig. 1. (a) Overall configuration of the contact zone between an individual disc cutter and rock, and (b) standard apparatus for measuring wear.

2.2. Assumptions governing the numerical simulation

According to Eq. (7), if F_r, F_n, and F_s can be accurately estimated, the disc cutter wear for any given geometry can be calculated. Since determining these forces in the rock-cutter interaction process involves a complex procedure, including the nonlinear behavior of materials, diverse boundary conditions, and dynamic impact, the explicit finite element method (ANSYS LS-DYNA) was selected for the simulation. The explicit finite element method is a widely used numerical approach for dynamic and nonlinear engineering problems. In this method, the discretized equations of motion are directly integrated using explicit time integration formulas, such that the values of numerical variables at each time step depend only on known quantities from the previous step. Compared to implicit methods, the explicit finite element method typically requires a very small time step to maintain numerical stability. However, due to the simplicity of calculations in each step, it is often more efficient for many problems involving a large number of degrees of freedom and nonlinear behavior. Provided that appropriate time increments are used, this method offers high stability and accurate results in analyzing transient phenomena with rapid time variations, such as impact, penetration, and contact problems. A review of the scientific literature shows that constant-stress hexahedral elements (Cho et al., 2013; Li and Du, 2016) and constant-stress tetrahedral elements (Jaime et al., 2015) have been used for simulating rock-cutter interactions. However, hexahedral elements provide better precision to estimate forces and wear (Rokhy et al., 2022).

Regarding element size, several researchers assert that, alongside accuracy and convergence, the element size in analyses with element erosion is constrained by the actual size of the rock particles (Bandini et al., 2014; Jaime et al., 2015; Norouzi et al., 2013). Cho et al. (2013), in modeling granite rock cutting, asserted that elements with a volume of 0.027 m^3 are adequately diminutive to guarantee the precision of numerical modeling. Accordingly, the elements of damaged zone under the cuter are refined to meet this criterion. Moving away from this critical zone, the elements gradually increase in size to reduce the runtime of the problem without significantly affecting solution accuracy. Finally, in the numerical simulation, the rock and the disc cutter were meshed with 570,240 (590,542 nodes) and 21,600 (25,680 nodes) hexahedral elements, respectively.

Relating to the dimensions of modeling excavated zone by cutter, Richard et al. (1998) have stated that the cutting force should be distributed in a distance at least one order of magnitude greater than the cutting depth. In other words, the horizontal dimension ratio (l) to the cutting depth (p) should observe the minimum ratio of $l/p \geq 10$. However, to achieve high accuracy and examine the variations in forces acting on dual disc cutters, the dimensions used in this study are chosen to be much larger than the minimum required size. Additionally, to closely match real conditions, the disc cutter dimensions are modeled according to reality (17-inch disc cutter). The dimensions of the numerical model are presented in Fig. 2. Since firstly the results of the numerical method have been compared with the results of LCM, the boundary conditions are set exactly as in previous studies (Cho et al., 2010, 2013; Li and Du, 2016). In other words, since in the LCM test the rock specimens were cast in concrete and then placed inside a steel chamber to ensure they remained fixed during testing, in the numerical simulation, the degrees of freedom on the side and bottom faces were also constrained. Furthermore, penetration depths of the disc cutter were set to two values: 4 mm and 8 mm, such that the spacing-to-penetration ratio (s/p) would be 5, 7.5, 10, 12.5, 15, and 20. Moreover, the rock specimen surfaces are defined as non-reflective boundaries, which allowing for the dissipation of stress waves. When it comes to the stress distribution close to the model corners non-reflective boundaries have no effect. Finally, before starting the analysis, gravitational load $g = 9.81$ m/s^2 is applied to the model.

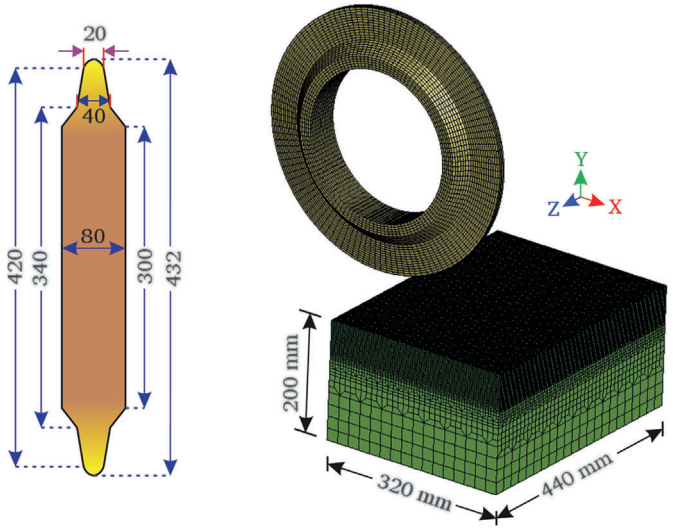

Fig. 2. Geometry and meshing of the rock sample along with the disc cutter in real dimensions (dimensions in mm).

2.3. Material constitutive model

The groove geometry through the rock cutting and applied force on cutter are directly dependent on the selected rock constitutive model. Furthermore, only the constitutive models are permitted for selection which can account for the influence of various factors, such as compressive strength, elastic modulus, and in-situ stresses, on the final results. Therefore, the shape of the damaged zone under the disc cutter and the applied forces serve as criteria for selecting the constitutive equations. To simulate the groove created by the disc cutter, the elements along this path must have the ability to be removed from the model in some way. Depending on the stress or strain state, element erosion can occur either in front of the disc cutter (mainly due to compressive failure of material) or across the rock surface due to fracture propagation. Although no general guidelines exist for selecting an element erosion criterion, the overall response of the simulation in the rock cutting process is highly sensitive to the value chosen for the erosion parameter. Therefore, selecting the appropriate parameter is a trial-and-error process to accurately model the applied forces on the disc cutter and the damaged zone. Ultimately, after numerous simulations, a strain-based criterion was selected for element erosion. This means that when the strain of any element reaches a specific value of 0.1, it is removed from the model. Based on the above criteria, four specific constitutive material models of geo-materials including Johnson Holmquist Concrete (JHC), Continues Surface Cap Model (CSCM), RHT, and Concrete Damage Rel3 are investigated in reproducing the results of uniaxial compressive strength and the forces acting on the disc cutter in the linear cutting test. Fig. 3 shows the applied forces on the disc cutter for each constitutive model used. In this figure, the JHC constitutive model demonstrates good agreement with the expected value. Therefore, the JHC constitutive model is approved for the next stage of modeling. In addition, the JHC model has the ability to investigate the influence of selected parameters on the applied forces on the disc cutter. The input parameters for the JHC model are also presented in Table 1. Although some research has shown that rocks have anisotropic and heterogeneous properties (Abbasi et al., 2024; Mohtarami et al., 2017, 2019, 2022), this issue has been ignored due to the simplification and closeness of the rock properties to the isotropic homogeneous state.

3. Determination of disc cutter forces

To support the proposed numerical method and constitutive equations, the forces acting on a single CCS disc cutter with a 17-inch

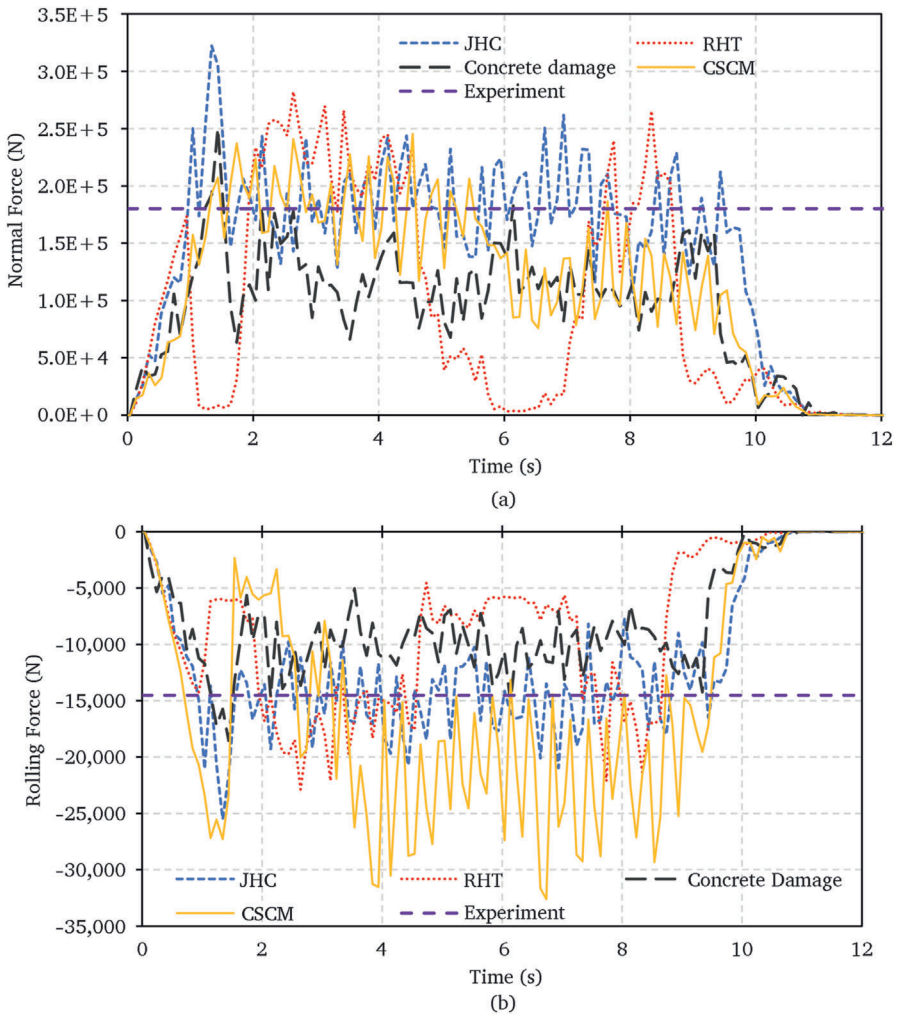

Fig. 3. Comparison of the results of different constitutive models in estimating the applied forces on the cutter with experimental results.

Table 1
Input parameters of constitutive models for the rock and disc cutter.

JHC parameters for rock			
Material Parameters		Damage parameters	
Density (kg/m^3)	2665	D_1	0.04
Shear modulus (MPa)	19,310	D_2	1.00
EOS parameters		Strength parameters	
P_c (MPa)	20.67	A	0.79
U_c	0.001	B	1.60
P_l (MPa)	800	C	0.007
U_l	0.11	N	0.61
K_1 (MPa)	85,000	Fc (MPa)	137.9
K_2 (MPa)	−171,000	T (MPa)	8.7
K_3 (MPa)	208,000	SFMAX	7
-	-	EPS0 (1/ms)	0.001
-	-	EFMIN	0.01
Disc cutter Parameters			
Density (kg/m^3)	7850	Poisson's ratio	0.3
Elastic modulus (GPa)	200	-	-

diameter during the cutting of Indiana Limestone, as conducted by Rostami (1997), are compared with the results of the numerical method. Fig. 4 shows the rolling forces (F_r), normal forces (F_n), and side forces (F_s) applied to the disc cutter. In this diagram, the solid lines represent the results of the numerical method, while the dashed lines indicate the experimental average values reported by Rostami (1997). It should be mentioned that Rostami (1997) measured only the normal and rolling forces experimentally (red dashed lines in Fig. 4a and b) and the side forces are considered equal to zero according to theory (yellow dashed line in Fig. 4c).

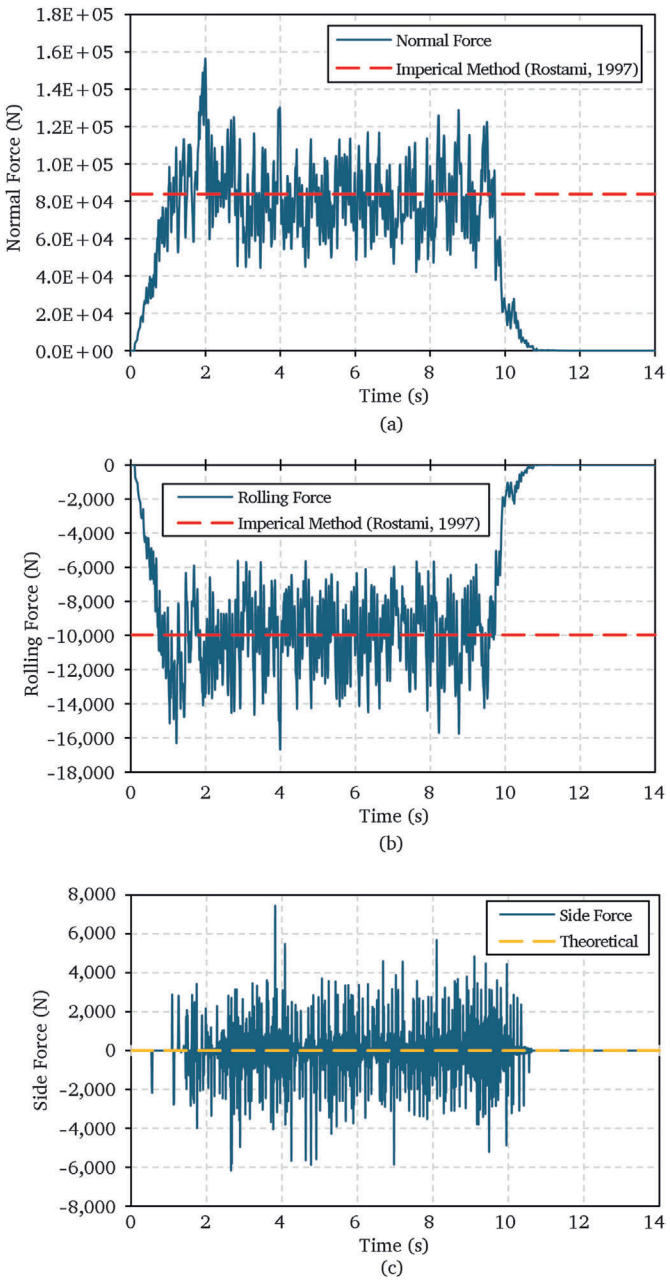

Fig. 4. Comparison of the numerical and experimental LCM (Rostami, 1997) methods for: (a) Rolling force, (b) normal force, and (c) lateral force, applied to the disc cutter at a penetration depth of 7.62 mm in Indiana Limestone.

In the double disc cutter condition, the applied forces on the second disc will be reduced due to the groove created by the first disc cutter. This reduction depends on the spacing of the disc cutters and the penetration depth (Cho et al., 2010). To confirm the mentioned hypothesis, a second stage of validation is conducted using the results from Cho et al. (2013), which are obtained from LCM tests on a granite sample and finite element simulations. The analytical part used the CSM method introduced by Rostami and Ozdemir (1993). Fig. 5 shows an example of the stresses induced in the rock and groove geometry resulting from boring by single and double disc cutters. The mechanical properties of the specimens are according to Cho et al. (2013). Table 2 compares the average absolute normal and rolling forces calculated by the suggested technique for different penetration depths and cutter spacings with those calculated by other techniques. It is evident, the proposed method shows good accuracy.

The analytical method (Rostami, 1997) and the approach of Cho et al. (2013) yield elevated values for the rolling force across all penetration depths, while the suggested method offers reasonable accuracy compared to LCM results. The discrepancy between the numerical and the theoretical solutions can be attributed to the simplifying assumptions in the analytical method (such as the distribution of forces beneath the cutter or the constancy of coefficients during the analysis). Based on the numerical simulation, at all penetration depths, both normal and sliding forces increase with greater cutter spacing; however, beyond a certain point (s/p around 15), no significant increase in applied forces is observed. This indicates that the interaction between adjacent cuts ceases, and each cut can be considered independently. This pattern is also evident in the LCM test outcomes. At shallow penetration depths, the analytical method overestimates the normal force, and as the penetration depth increases, this method underestimates the force. In contrast, the suggested technique demonstrates good concordance with LCM test results.

4. Numerical investigation of effective parameters on wear

As previously mentioned, the disc cutter wear rate changes as the cutter wears down. This phenomenon can be attributed to the change in the geometry (becoming wider) of the cutter tip and the material mechanical properties. Considering this point, calculating disc cutter wear using the numerical method is a time-dependent simulation where geometry and mechanical properties must be updated during excavation. Therefore, the forces on a new disc are first calculated using the specified C_H coefficient, and then the volumetric wear is computed using Eq. (7). After that, the disc cutter's geometry and C_H coefficient are updated, and the wear calculation is repeated. The more frequently this update occurs, the more accurately the wear is estimated. Eq. (7) provides the volumetric wear of the disc cutter. However, in practice, operators measure radial wear using special stencils. Radial wear refers to the reduction in the disc cutter's radius due to wear and is quantified in millimeters. By having the precise geometry of the cutter and assuming uniform wear, volumetric wear can be converted into radial wear. The cutter geometry is subsequently updated based on the computed wear, and the forces on the worn disc are recalculated for the next cutting interval. This procedure persists until the radial wear reaches a critical threshold, which causes cutter lose its efficiency. When the wear reaches this critical level, the disc cutter is replaced. The manufacturer suggests this critical wear level to be 25 mm. Therefore, in this section, the lifespan of a cutter installed at a 2-m radius (R_i = 2 m) is predicted numerically under normal and inclined conditions, with three uniaxial compressive strengths (σ_c = 31, 62.1, 137.9 MPa), three elastic moduli (E = 30, 47.5, 65 GPa), three penetration depths (P = 2.54, 5.08, 7.62 mm), and various confining stresses (σ_x-σ_z = 0-0, 5-5, 15-15, 5-15, 15-5 MPa). It is worth mentioning, since to verify the numerical model, it is necessary to compare the results with another method, the numbers related to σ_c, E, and P are adopted from Rostami (1997). These values represent three types of weak, medium, and strong rocks, and a linear cutting test was performed on them with the aforementioned penetration depths.

It should be noted that the actual path of disc cutters is circular. Theoretically, the difference between circular and linear paths lies in the magnitude of side forces, as the resultant of side forces in circular paths is non-zero. This may lead to increased abnormal wear in cutters traversing small-diameter circles (center discs). However, as the distance from the center of the cutterhead increases, the forces on the disc cutters converge to the results of linear cutting tests (Deng et al., 2024). Since this study only considers normal wear, the circular path has been disregarded in the single-disc simulation section (Section 4). Furthermore, as shown in Table 2, cutter spacing is one of the factors affecting the applied forces on the disc cutter. However, due to previous studies (Cho et al., 2010, 2013; Gertsch et al., 2007; Li and Du, 2016) on this parameter and the emphasis of this study on geomechanical factors,

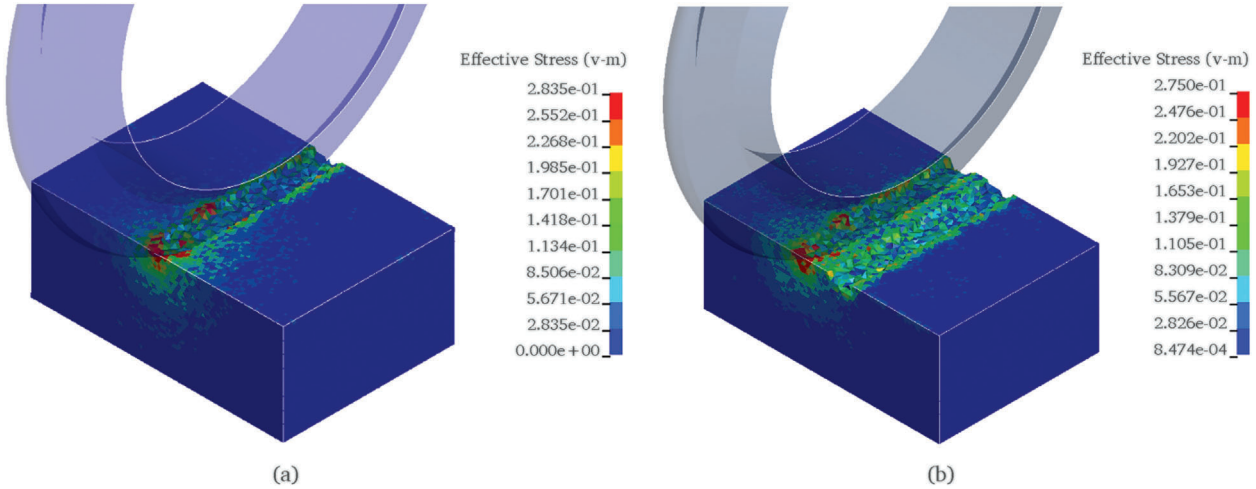

Fig. 5. Effective stresses (in GPa) applied on the rock specimen excavated by: (a) a single disc cutter, and (b) dual disc cutters.

Table 2
Comparison of the results from different methods for estimating normal and rolling applied forces on the disc cutter at various penetration depths and cutter spacings.

P (*mm*)	*S/P*	Mean rolling forces (kN)				Mean normal forces (kN)		
		LCM (Cho et al., 2013)	Analytical (Rostami, 1997)	FEM (Cho et al., 2013)	Presented method	LCM (Cho et al., 2013)	Analytical (Rostami, 1997)	Presented method
4	5	3.7	13.31	5.3	3.91	99.2	137.67	109.66
	7.5	5.5	13.68	6.3	5.13	119.2	141.49	122.32
	10	5.8	14.05	7.1	6.20	122	145.31	129.73
	12.5	6.3	14.42	7.8	7.68	127.7	149.13	134.07
	15	–	14.79	8.2	7.79	–	152.95	141.27
	20	5.7	15.53	8.1	7.67	147.4	160.59	140.86
8	5	13.2	20.50	19.4	9.97	167.2	149.19	163.81
	7.5	17.2	21.55	20.3	11.64	212.5	156.83	198.77
	10	17.3	22.60	21.4	13.95	219.3	164.47	207.51
	12.5	–	23.65	23.5	14.39	–	172.12	212.49
	15	17.6	24.70	24.6	16.06	234.6	179.76	218.75
	20	17.2	26.80	26.2	16.15	228.7	195.04	219.14

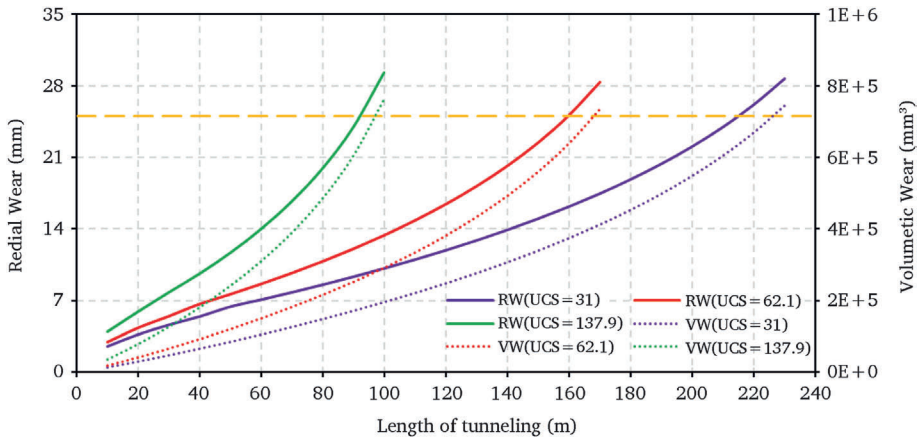

Fig. 6. Variation of volumetric wear (VW) and radial wear (RW) of the disc cutter versus tunnel length ($R_i = 2\ m$). The yellow dashed line indicates the critical wear level of 25 mm (according to the manufacturers' suggestion), indicating the threshold for disc cutter replacement.

separate investigation of this factor has been omitted. Nevertheless, in Section 5, the effects of both the circular path of disc cutters and their spacing have been investigated through full-scale cutterhead simulation.

4.1. Impact of rock compressive strength on disc cutter wear

To examine the wear of disc cutters in rocks with different compressive strengths, three different values of σ_c are selected, representing weak rocks (σ_c = 31 MPa), medium-strength rocks ($\sigma_c = 62.1$ MPa), and strong rocks ($\sigma_c = 137.9$ MPa). The elastic modulus is kept constant at $E = 47.5$ GPa, with a penetration depth of 5.08 mm, and the sample is simulated without any confining stress. Fig. 6 also illustrates the radial and volumetric wear of the disc cutter positioned 2 m from the center of the cutterhead. As expected, both types of wear

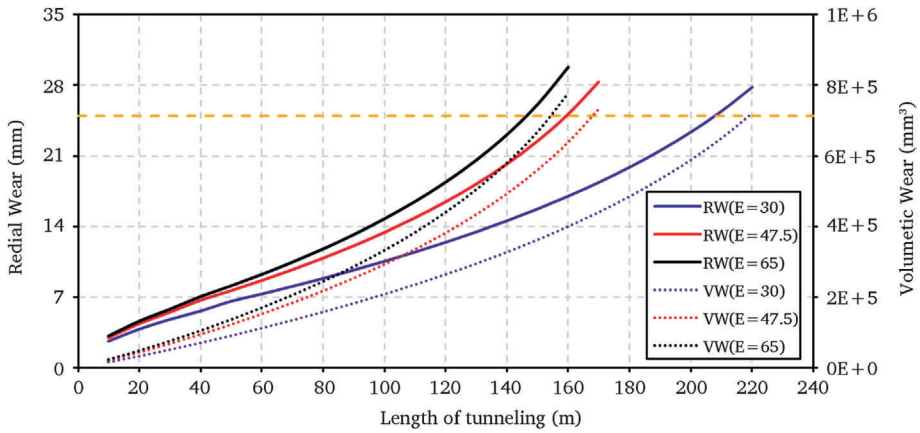

Fig. 7. Variation of volumetric wear (VW) and radial wear (RW) of the disc cutter positioned at a 2-m cutterhead radius versus length of tunneling.

increase with the length of the tunnel excavation. For volumetric wear, the increasing trend starts slowly and linearly. However, as wear continues, applied forces increase and finally, by reducing the hardness of the cutter, the trend has increased non-linearly and exponentially. Similarly, radial wear increases at a slow rate initially, with the concavity of the graph facing downward in the early stages. This is due to the design of CCS disc cutters and is considered one of their advantages (Sun et al., 2023). However, as wear progresses, the rate of disc cutter wear accelerates, and the concavity of the graph turns upward. This graph indicates that once the wear surpasses a critical level, the disc cutter loses its efficiency and must be replaced.

4.2. Impact of rock elastic modulus on disc cutter wear

In an experimental investigation on disc cutter wear, Rostami (1997) predicted that the rock elastic modulus can significantly influence wear. However, a comprehensive study on the extent of the impact of rock elastic modulus on disc cutter wear has not yet been conducted. To investigate this, the uniaxial compressive strength (σ_c = 62.1 MPa), penetration depth (P = 5.08 mm), and confining stresses (σ_x, σ_y = 0 MPa) are kept constant, while three different values of elastic modulus (E = 30, 47.5, 65 GPa) are assigned to the rock. Fig. 7 illustrates the wear of the disc cutter positioned at a 2-m distance from the cutterhead center. Fig. 7 displays a similar trend as Fig. 6 for both volumetric and radial wear. However, the intensity of disc cutter wear changes with the elastic modulus is not as significant as with uniaxial compressive strength. In other words, the impact of the elastic modulus on wear is less pronounced than that of σ_c. When the elastic modulus increases from 30 to 45.5 GPa, the increase in wear is considerably more than when the modulus rises from 45.5 to 60 GPa. This can be attributed to the brittleness of the rock.

4.3. Impact of penetration depth on disc cutter wear

Penetration depth constitutes a critical parameter influencing the applied forces and the disc cutter wear, and it has been extensively studied in previous research (Cho et al., 2013; Gertsch et al., 2007; Li and Du, 2016). In this section, with the uniaxial compressive strength (σ_c = 62.1 MPa), elastic modulus (E = 47.5 GPa), and confining stresses (σ_x, σ_y = 0 MPa) kept constant, three different penetration depths (P = 2.54, 5.08, 7.62 mm) are considered. Fig. 8 shows the normal, rolling, and lateral forces acting on a wear-free disc cutter at the aforementioned penetration depths. The sharp increase in forces at the initial stage is due to the sudden contact of the disc cutter with the rock sample. It is important to note that this peak is not included in the averaging process. Under these conditions, and for excavating 10 m of the tunnel, the volumetric wears of a disc cutter positioned at a distance of 2-m from the center of the cutterhead are calculated to be 15,212.44 m^3, 19,245.84 m^3, and 33,118.58 m^3 for penetration depths of 2.54 mm, 5.08 mm, and 7.62 mm, respectively. While the corresponding radial wears are calculated to be 2.61 mm, 2.93 mm, and 3.85 mm, respectively. Although penetration depth directly influences the increase in forces on the disc cutter, it cannot be concluded that a lower penetration rate necessarily means less wear and a more economical operation. For a given tunneling length, with smaller penetration depths, the disc cutters will traverse a greater distance, which may ultimately lead to increased cutter wear. Therefore, the penetration depth should be optimized based on the existing conditions and the applied forces. In a specific length of tunneling in weak rock (σ_c = 31 MPa), in most cases, the wear on the disc cutter increases in tandem with the penetration depth. However, this procedure changes with the increase in rock strength. For example, in 10 m tunnel excavation in strong rock (σ_c = 137.9 MPa, E = 65 GPa) with confining pressure of σ_x = 5 MPa, σ_y = 5 MPa, the radial wear is calculated as 2.74 mm, 3.25 mm, and 3.16 mm for penetration depths of 2.54, 5.08, and 7.62 mm, respectively.

4.4. Impact of confining stress on disc cutter wear

To examine the influence of confining stresses on the wear of disc cutters, the uniaxial compressive strength (σ_c = 62.1 MPa), the rock elastic modulus (E = 47.5 GPa), and the penetration depth (P = 5.08 mm) are kept constant, while different values of confining stresses (σ_X-σ_Z = 0-0, 5-5, 15-15, 5-15, 15-5 MPa) are applied to the rock specimen. As shown in Fig. 2, the x-axis represents the cutting direction, the z-axis is perpendicular to it, and the y-axis is aligned with the disc cutter's penetration direction, representing the tunnel face (σ_y = 0). Fig. 9 shows the disc cutter wear versus tunnelling distance under different confining stresses. According to this figure, increasing the confining stress results in a relatively small increase in wear. When the confining stress changes from 0 to 0 to 5-5, the cutter life decreases by approximately 3 m. However, the change from 5 to 5 to 15-5 does not show a significant impact on wear. Yet, when the 5-15 stresses are applied to the sample, again a noticeable increase in wear is observed. Nevertheless, wear under 15-15 confining stresses shows a trend somewhat similar to 5-15. This result indicates that the confining stress perpendicular to the cutting direction (in this case, σ_z) plays a more critical role than the confining stress in the cutting direction (in this case, σ_x). This finding was also reported by Ma et al. (2016) using LCM. However, it is important to note that the actual trajectory of the disc cutter in a TBM is circular, and the direction of confining stresses relative to the cutting path is continuously changing. Therefore, it is recommended to use the average stress in wear calculations. Table 3 shows the average estimated numerical results for the forces acting on the cutter along with the lifespan of disc cutters at different confining

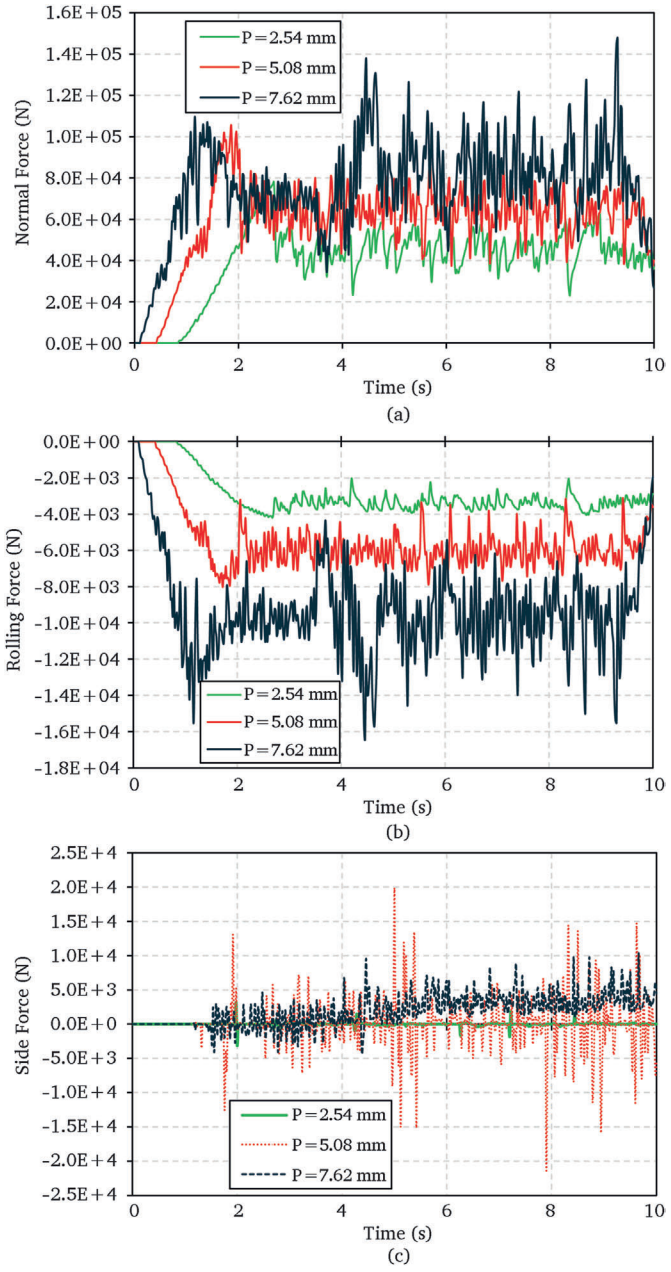

Fig. 8. Applied forces on a wear-free disc cutter: (a) normal forces, (b) rolling forces, (c) side forces; for penetration depths of 2.54 mm, 5.08 mm, and 7.62 mm.

stresses. Although the confining stresses directly affect the normal force, the rolling force shows fluctuations that can be attributed to the crushing of the rock in front of the cutter due to compressive stress.

4.5. Impact of disc cutter angle on wear

To achieve a consistent tunnel profile, the peripheral disc cutters of a TBM are installed at an inclined angle. This section aims to compare the wear of an inclined disc cutter with a 20° angle to that of a vertically aligned disc cutter. Therefore, the uniaxial compressive strength, elastic modulus, and penetration depth (P = 5.08 mm) are kept constant, and the disc cutters are evaluated without any confining stresses. The wear of the disc cutter positioned 2 m from the center of the cutterhead, either at a normal or inclined angle, is calculated. It is important to note that

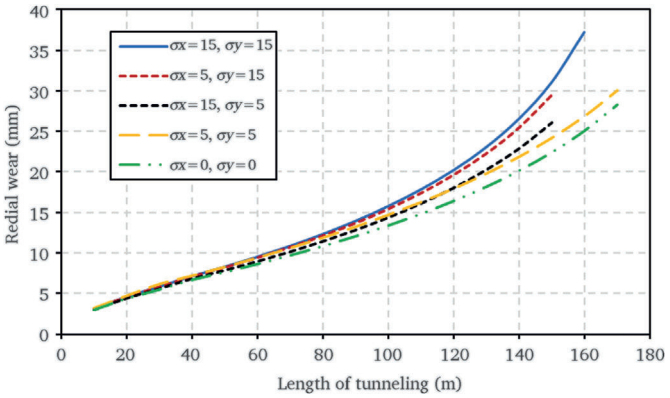

Fig. 9. Estimated cutter life as a function of tunnelling distance under different confining stresses.

Table 3
Numerical estimation of average forces and cutter life under different confining stresses.

$\sigma_x - \sigma_y$	Ave. F_n (kN)	Ave. F_r (kN)	Ave. F_s (kN)	Disc Cutter life (m)
0–0	63.790	−5.932	0.053	160.196
5–5	77.034	−7.223	−0.154	153.594
15–15	97.018	−6.969	0.020	135.989
5–15	91.951	−6.433	0.000	138.631
15–5	86.755	−6.815	−0.032	146.553

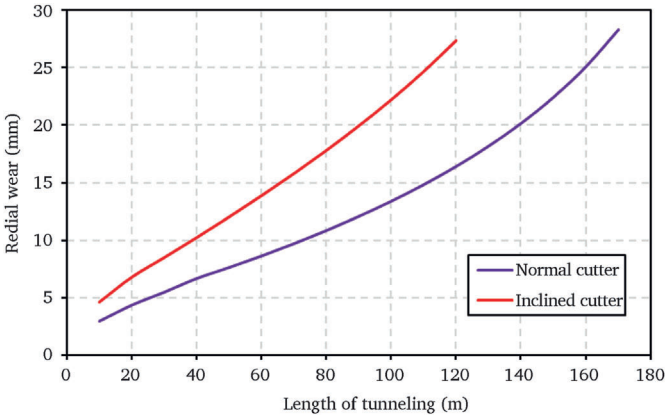

Fig. 10. The impact of disc cutter inclination angle on wear.

while the normal and rolling forces on the inclined disc cutter are less than those on the vertical cutter, the lateral force increases significantly. Fig. 10 compares the lifespan of the two aforementioned disc cutters. As shown, the wear of the inclined cutter is significantly greater than that of the vertical cutter, resulting in a shorter lifespan. This increased wear can be attributed to the higher lateral forces. It should be noted that in practice, these disc cutters experience uneven wear, although such a condition was not considered in this simulation.

5. Full-scale simulation of disc cutter wear

Given that the actual trajectory of the disc cutters in operation is circular and that their installation position and spacing also influence their wear, this section provides a more detailed modeling of mechanized tunneling with a TBM. The simulation is compared and supported using the results from the Gelas water conveyance tunnel project.

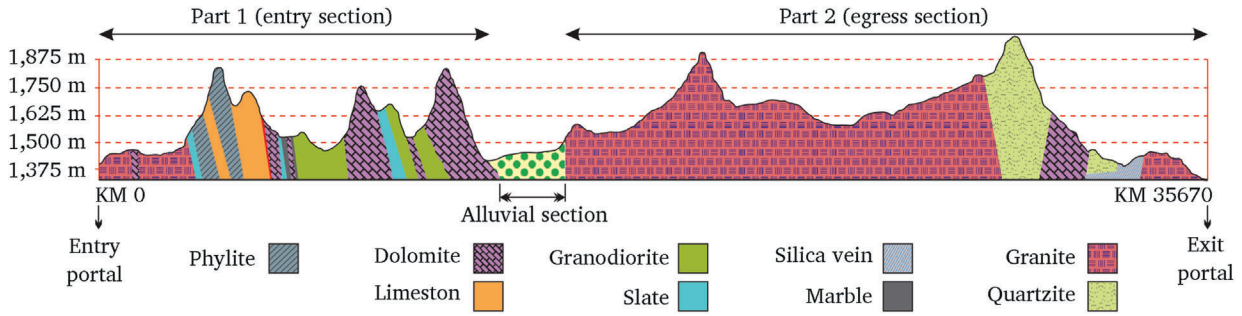

Fig. 11. The various geological structural zones along the Gelas water transfer tunnel.

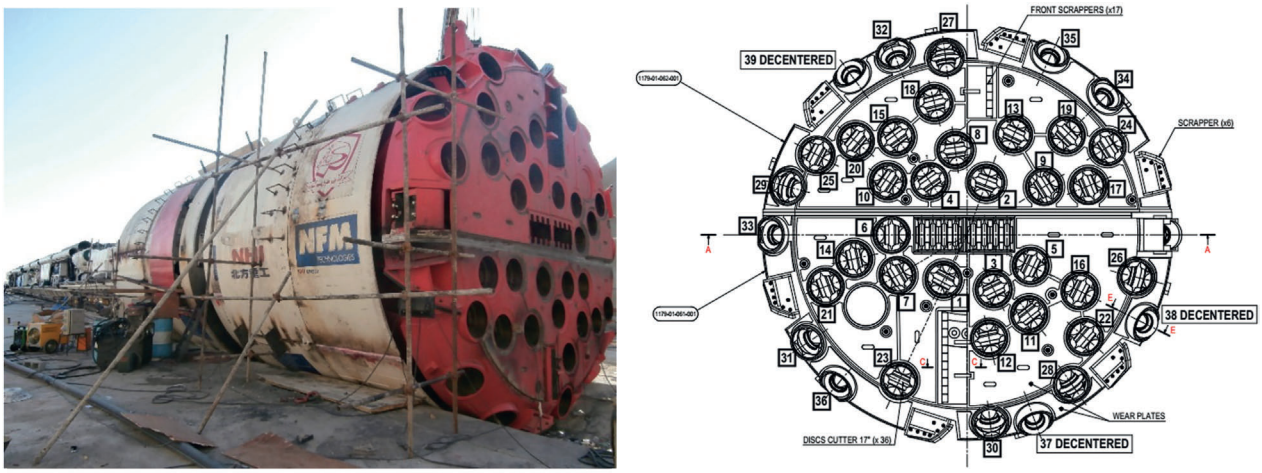

Fig. 12. (a) TBM used at the Gelas water transfer tunnel; (b) Configuration of the disc cutters on the cutterhead.

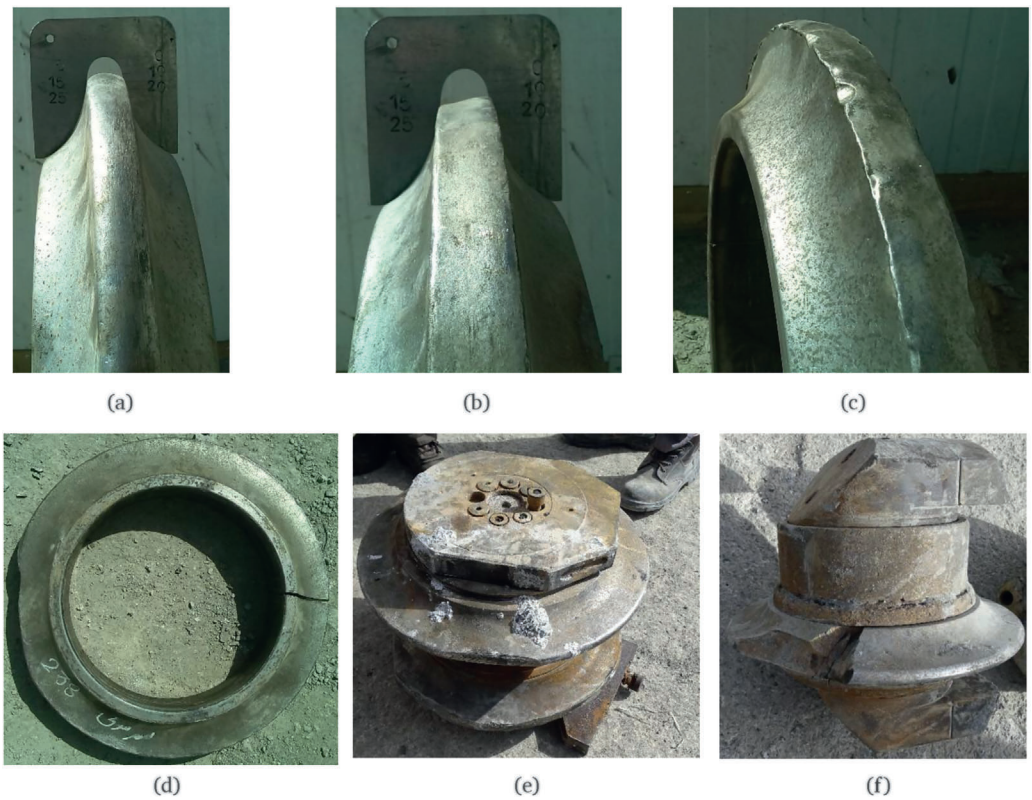

Fig. 13. Various disc cutter wear and failure patterns: (a) normal wear, (b) uneven wear, (c) edge curling or mushrooming, (d) cutter ring fracture, (e) disc cutter offset grinding, and (f) bearing damage and ring displacement.

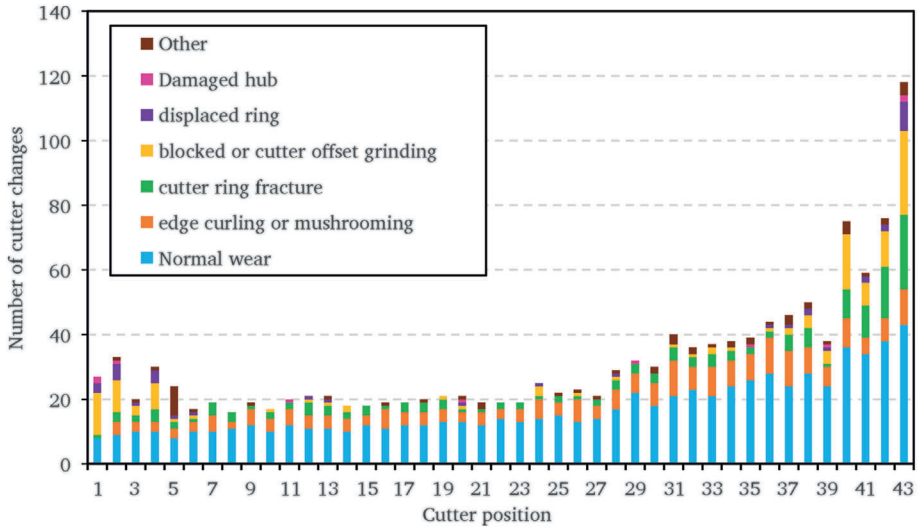

Fig. 14. Number and reasons for disc cutter replacements in the Gelas water conveyance tunnel project based on their position on the cutterhead.

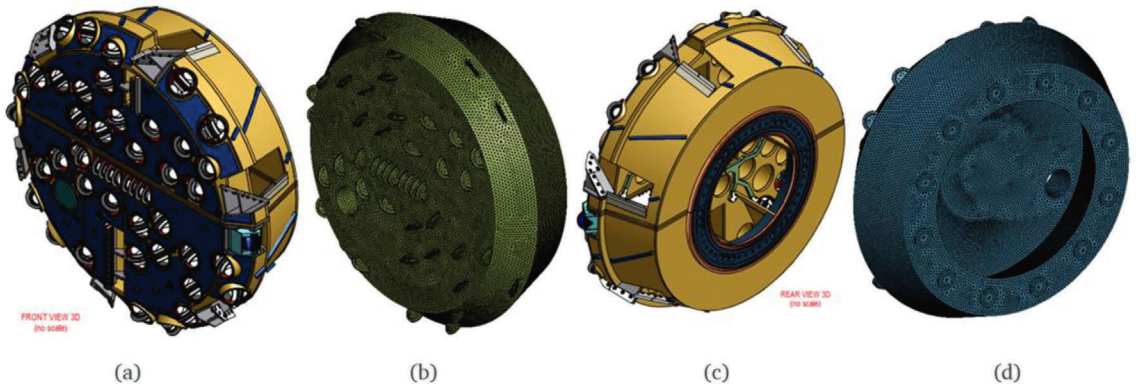

Fig. 15. 3D schematic and numerical model of the cutterhead: (a) front view, (b) numerical model showing the layout of the disc cutters, (c) rear view, and (d) numerical model showing the layout of the jacks.

5.1. Project overview

The Gelas water conveyance tunnel, with a length of 35,661 m in northwest Iran, was excavated utilizing two TBMs with a diameter of 6.325 m. The disc cutters used in the TBM were 17 inches in diameter. Geological studies indicated that the majority of the tunnel is composed of igneous rocks (Fig. 11). During the excavation, operational data, geological and geomechanical information, and details regarding disc cutter replacements were recorded in a comprehensive database. A view of the TBM and the arrangement of the disc cutters on the cutterhead is shown in Fig. 12.

In addition to normal wear, the reasons for disc cutter replacements included edge curling or mushrooming, cutter ring crack, bearing damage, ring displacement, and uneven wear (Fig. 13). Fig. 14 illustrates the quantity and reasons for each cutter replacement in relation to their position on the cutterhead. It should be noted that normal wear refers to wear that reduces the disc cutter radius from the outside toward the core in almost the same way at all points. According to Fig. 14, this type of wear takes up most of the replacements and includes 54.5% of them. In this study, only normal wear is considered in the calculations because of the existing complexities. Therefore, by identifying the disc cutters substituted owing to normal wear, the lifespan of all disc cutters (in terms of tunnel excavation kilometers) relative to their location on the cutterhead can be calculated. These values were used for comparison with the numerical results.

5.2. Investigating the impact of disc cutter position on wear

To examine the impact of the rotational movement of the disc cutters, along with their positioning and installation angle on wear, the TBM used in the Gelas water conveyance tunnel project is modeled in full scale. Fig. 15 shows a schematic of the cutterhead and the constructed numerical model in 3D. As indicated, the arrangement of the disc cutters and the location of the machine's jacks are modeled exactly as in reality.

After constructing the numerical model of the cutterhead, a rock segment with dimensions of 10,320 mm, 10,320 mm, and 3000 mm in length, width, and thickness, respectively, with specific uniaxial compressive strength (σ_c = 88.1 MPa) and elastic modulus (E = 48.3 GPa), and without confining stresses, is modeled according to the rock properties of the tunnel. The cutterhead model consisted of 1,078,590 tetrahedral elements, while the rock model used 576,000 hexahedral elements. Fig. 16a and d shows the Von Mises stresses in the rock at different stages of excavating. The stresses generated by the contact between the disc cutters and the rock are clearly visible. Fig. 16e illustrates the lateral forces applied on the cutterhead, which, as expected, oscillated around zero. Fig. 16f shows the force applied to the cutterhead in the boring direction or the machine's thrust. The fluctuations in this graph can be attributed to the machine's cyclical advancement. The operational data related to the machine's thrust were recorded between 3565 kN and 12,667 kN, showing good agreement with the numerical model.

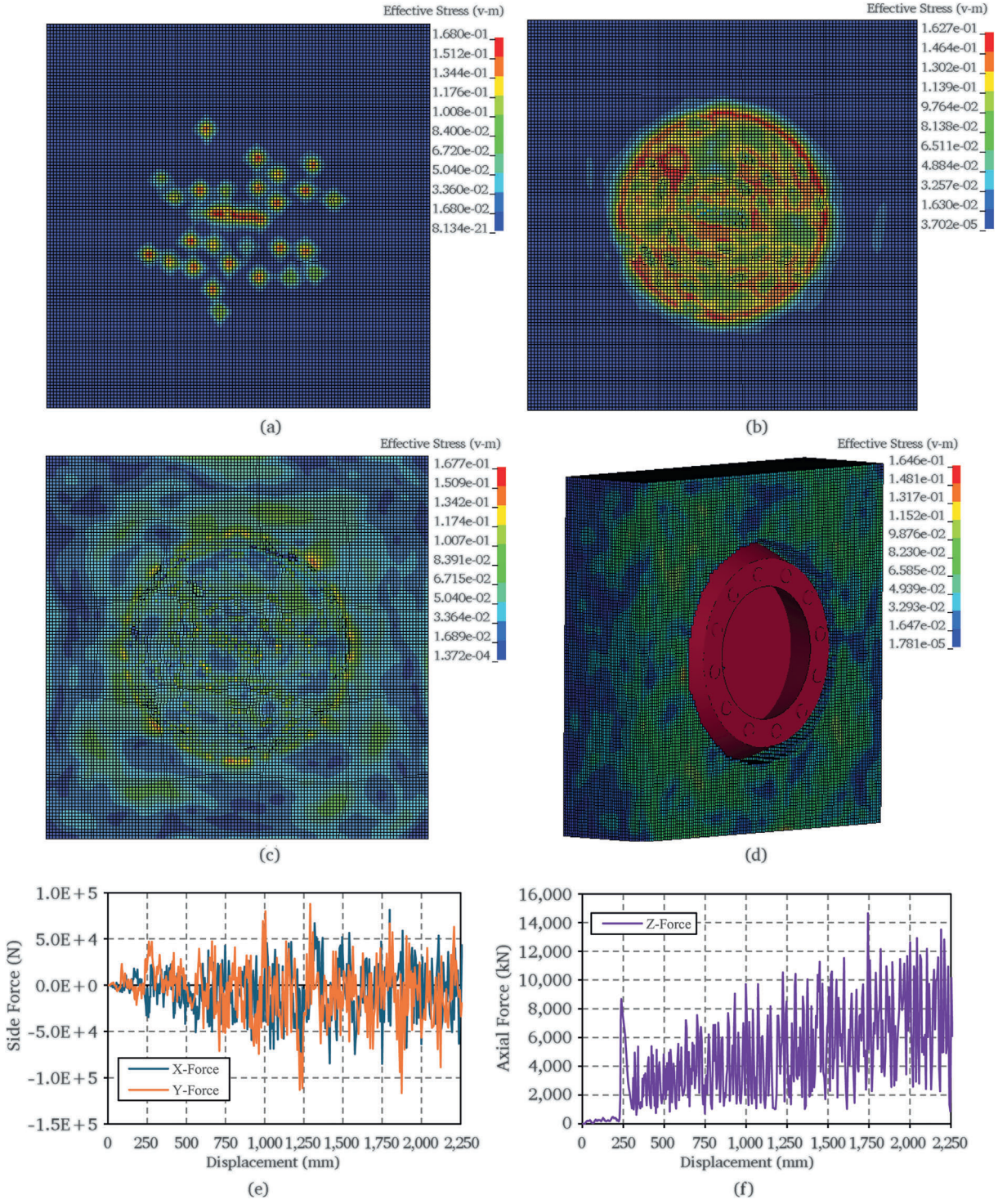

Fig. 16. Von Mises stresses in the rock at various stages of excavating: (a) initial stage, (b) mid-stage, (c) advanced stage, (d) final stage, (e) lateral forces acting on the cutterhead, and (f) force applied in the boring direction (thrust).

A comparison of numerical results and actual data for the disc cutter life versus its position is shown in Fig. 17. Based on this figure, it can be understood that the numerical estimations for the central disc cutters generally exceed the actual values, while they show reasonable accuracy for the middle disc cutters. Finally, the numerical estimations for the peripheral disc cutters tend to be somewhat lower than the actual values. The absolute error magnitude for the central disc cutters (8 pieces), face disc cutters (25 pieces), and peripheral disc cutters (10 pieces), is 20.45%, 14.66%, and 11.67%, respectively.

6. Conclusion

Advance rate and productivity in mechanized drilling method is directly dependent on cutting tool efficiency. Without considering disc cutter wear estimation of final time and cost does not have sufficient accuracy. Therefore, in this study, a comprehensive numerical simulation is conducted to evaluate the wear of disc cutters and verified by results of previous research and field results. The impact of various factors, including compressive strength, elastic modulus, penetration

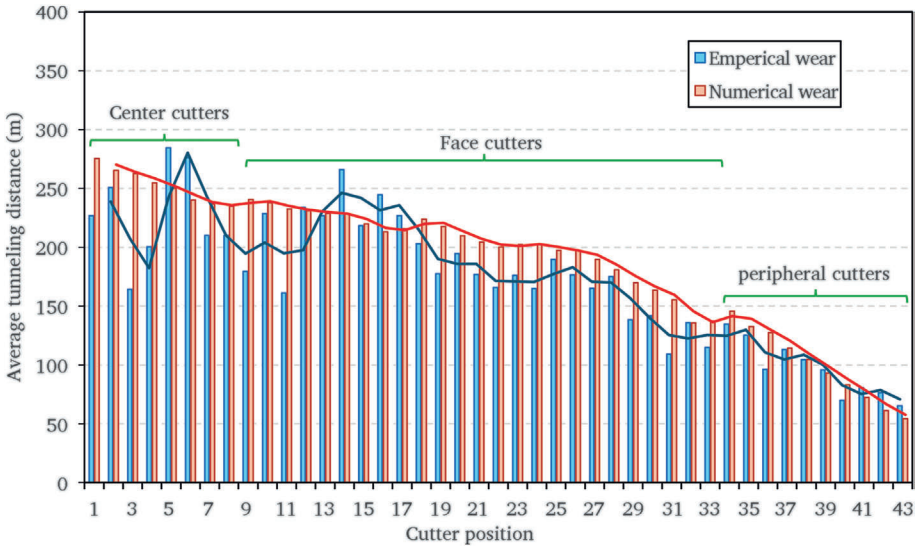

Fig. 17. Comparison of numerical results and real data for cutter life relative to disc cutter position.

depth, confining stresses, and disc cutter angle, on the wear of disc cutter is systematically investigated. The most important findings are listed as follows,

- Disc cutter wear increases significantly with the compressive strength of the rock. As the compressive strength rises, the rate of wear becomes more pronounced, particularly in harder rocks.
- Although the elastic modulus does not affect the wear of the disc cutter as much as the rock compressive strength, the increase of the elastic modulus causes the wear of the cutter to increase. It is worth noting that the rate of wear increase diminishes at higher moduli.
- While penetration depth directly influences the increase in forces on the disc cutter, it cannot be concluded that a lower penetration rate necessarily means less wear and a more economical operation. The overall disc cutter travel distance increases with smaller penetration depths, potentially leading to greater wear. Therefore, the penetration depth should be optimized based on the existing conditions and the applied forces.
- According to numerical results, increasing the confining stress results in a relatively small increase in wear. However, specimens under confining stresses showed significant wear compared to free specimens. The rate of increase in wear became slower with the increase of confining stresses, though. Results indicate that the confining stress perpendicular to the direction of cutting plays a more critical role than the confining stress in the cutting direction. According to the rotary path of Cutterhead, it is suggested to use average stress in wear calculations.
- Inclined disc cutters experience significantly higher wear compared to vertical disc cutters, primarily due to the increased lateral forces. This results in a shorter lifespan for inclined disc cutters.

The current study is focused on the wear of disc cutters in hard rock, because the tunneling boring mechanism is different in soil and alluvial environments and tool wear is not one of the basic problems. On the other hand, only the normal wear of cutters (which includes a significant part of replacements) is considered in the modeling. Although in Sec. 4, the numerical results are investigated for the disc located 2 m away from the cutterhead's center, the full-scale simulation of the TBM cutterhead (Section 5) provided valuable insights into the relationship between disc cutter position and wear. The numerical estimates for disc cutter wear were generally consistent with field data, though some discrepancies were observed, particularly for central and peripheral disc cutters. The error analysis showed that the proposed method provides reasonable accuracy compared to the previous methods. Finally, it should be mentioned that the modeling was done for an isotropic homogeneous rock environment. While rock mass often has heterogeneous and anisotropic mechanical properties. In addition, the proximity of hard and soft rocks increases wear, which will be investigated in future studies by the authors. Overall, this study highlights the importance of considering various geomechanical and operational factors when predicting disc cutter wear and emphasizes the need for continuous monitoring and optimization to ensure efficient and cost-effective tunneling operations.

CRediT authorship contribution statement

Ehsan Mohtarami: Software, Methodology, Formal analysis, Conceptualization. **Amin Hekmatnejad:** Validation, Supervision, Investigation. **Georg H. Erharter:** Writing – review & editing, Writing – original draft, Conceptualization. **Alvaro Pena:** Writing – review & editing, Supervision, Project administration.

Declaration of competing interest

The authors declare that they have no known competing financial interests or personal relationships that could have appeared to influence the work reported in this paper.

Acknowledgements

The second author acknowledges the funding of the Agencia Nacional de Investigación y Desarrollo (ANID), through grant project of Fondecyt Iniciación No. 11221093.

References

Abbasi, V., Ahmadi, M., Mohtarami, E., Karimi, J., Saberi, F., 2024. Experimental and numerical failure mechanism evaluation of anisotropic rocks using extended finite element method. Theor. Appl. Fract. Mech. 131, 104411. https://doi.org/10.1016/j.tafmec.2024.104411.

Agrawal, A.K., Chattopadhyaya, S., Murthy, V.M.S.R., 2021. Delineation of cutter force and cutter wear in different edge configurations of disc cutters – an analysis using discrete element method. Eng. Fail. Anal. 129, 105727. https://doi.org/10.1016/j.engfailanal.2021.105727.

Bandini, A., Paolo, B., Bemporad, E., Sebastiani, M., Chicot, D., 2014. Role of grain boundaries and micro-defects on the mechanical response of a crystalline rock at multiscale. Int. J. Rock Mech. Min. Sci. 71, 429–441. https://doi.org/10.1016/j.ijrmms.2014.07.015.

Bruland, A., 2000. Hard Rock Tunnel Boring. NTNU, Trondheim, Norway.

Chang, S.H., Choi, S.W., Bae, G.J., Jeon, S., 2006. Performance prediction of TBM disc cutting on granitic rock by the linear cutting test. Tunn. Undergr. Space Technol. 21, 271. https://doi.org/10.1016/j.tust.2005.12.131.

Cho, J.-W., Jeon, S., Jeong, H.-Y., Chang, S.-H., 2013. Evaluation of cutting efficiency during TBM disc cutter excavation within a Korean granitic rock using linear-cutting-machine testing and photogrammetric measurement. Tunn. Undergr. Space Technol. 35, 37–54. https://doi.org/10.1016/j.tust.2012.08.006.

Cho, J.W., Jeon, S., Yu, S.H., Chang, S.H., 2010. Optimum spacing of TBM disc cutters: a numerical simulation using the three-dimensional dynamic fracturing method. Tunn. Undergr. Space Technol. 25, 230–244. https://doi.org/10.1016/j.tust.2009.11.007.

Deng, L.-C., Li, X.-Z., Xu, W., Zhang, C., Zhuang, Q.-W., Li, F.-Q., Zhou, Q., 2024. Full-scale test of disc cutter rotary cutting in TBM tunnelling: a case study of Mawan granite in Shenzhen, China. Geomech. Geophys. Geo-Energ. Geo-Resour. 10, 167. https://doi.org/10.1007/s40948-024-00886-3.

Erharter, G.H., Goliasch, R., Marcher, T., 2023. On the effect of shield friction in hard rock TBM excavation. Rock Mech. Rock Eng. 56, 3077–3092. https://doi.org/10.1007/s00603-022-03211-0.

Espallargas, N., Jakobsen, P.D., Langmaack, L., Macias, F.J., 2015. Influence of corrosion on the abrasion of cutter steels used in TBM tunnelling. Rock Mech. Rock Eng. 48, 261–275. https://doi.org/10.1007/s00603-014-0552-6.

Gehring, K., 1995. Prognosis of advance rates and wear for underground mechanized excavations. Felsbau 13, 439–448.

Gertsch, R., Gertsch, L., Rostami, J., 2007. Disc cutting tests in Colorado red granite: implications for TBM performance prediction. Int. J. Rock Mech. Min. Sci. 44, 238–246. https://doi.org/10.1016/j.ijrmms.2006.07.007.

Gong, Q.M., Jiao, Y.Y., Zhao, J., 2006a. Numerical modelling of the effects of joint spacing on rock fragmentation by TBM cutters. Tunn. Undergr. Space Technol. 21, 46–55. https://doi.org/10.1016/j.tust.2005.06.004.

Gong, Q.M., Zhao, J., 2009. Development of a rock mass characteristics model for TBM penetration rate prediction. Int. J. Rock Mech. Min. Sci. 46, 8–18. https://doi.org/10.1016/j.ijrmms.2008.03.003.

Gong, Q.M., Zhao, J., Hefny, A.M., 2006b. Numerical simulation of rock fragmentation process induced by two TBM cutters and cutter spacing optimization. Tunn. Undergr. Space Technol. 21, 263. https://doi.org/10.1016/j.tust.2005.12.124.

Gong, Q.M., Zhao, J., Jiao, Y.Y., 2005. Numerical modeling of the effects of joint orientation on rock fragmentation by TBM cutters. Tunn. Undergr. Space Technol. 20, 183–191. https://doi.org/10.1016/j.tust.2004.08.006.

Goryacheva, I.G., Goryachev, A.P., 2006. The wear contact problem with partial slippage. J. Appl. Math. Mech. 70, 934–944. https://doi.org/10.1016/j.jappmathmech.2007.01.010.

Hassanpour, J., Rostami, J., Tarigh Azali, S., Zhao, J., 2014. Introduction of an empirical TBM cutter wear prediction model for pyroclastic and mafic igneous rocks; a case history of Karaj water conveyance tunnel, Iran. Tunn. Undergr. Space Technol. 43, 222–231. https://doi.org/10.1016/j.tust.2014.05.007.

Hassanpour, J., Rostami, J., Zhao, J., Azali, S.T., 2015. TBM performance and disc cutter wear prediction based on ten years experience of TBM tunnelling in Iran. Geomech. Tunn. 8, 239–247. https://doi.org/10.1002/geot.201500005.

Huq, M.Z., Celis, J.P., 2002. Expressing wear rate in sliding contacts based on dissipated energy. Wear 252, 375–383. https://doi.org/10.1016/S0043-1648(01)00867-5.

Innaurato, N., Oggeri, C., Oreste, P.P., Vinai, R., 2007. Experimental and numerical studies on rock breaking with TBM tools under high stress confinement. Rock Mech. Rock Eng. 40, 429–451. https://doi.org/10.1007/s00603-006-0109-4.

Jaime, M.C., Zhou, Y., Lin, J.-S., Gamwo, I.K., 2015. Finite element modeling of rock cutting and its fragmentation process. Int. J. Rock Mech. Min. Sci. 80, 137–146. https://doi.org/10.1016/j.ijrmms.2015.09.004.

Jian, S., Peng, Z., Yuhou, W., Jinmei, Y., Defang, Z., Min, L., 2015. Stress and wear analysis of the disc cutter of rock tunnel boring machine. Open Mech. Eng. J. 9, 721–725. https://doi.org/10.2174/1874155X01509010721.

Jing, L-j, Li, J-b, Zhang, N., Chen, S., Yang, C., Cao, H-b, 2021. A TBM advance rate prediction method considering the effects of operating factors. Tunn. Undergr. Space Technol. 107, 103620. https://doi.org/10.1016/j.tust.2020.103620.

Johnson, K.L., 1985. Contact Mechanics. Cambridge university press, Cambridge.

Li, F.H., Cai, Z.X., Kang, Y.L., 2011. A theoretical model for estimating the wear of the disc cutter. Appl. Mech. Mater. 90–93, 2232–2236. https://doi.org/10.4028/www.scientific.net/AMM.90-93.2232.

Li, H., Du, E., 2016. Simulation of rock fragmentation induced by a tunnel boring machine disk cutter. Adv. Mech. Eng. 8, 1–11. https://doi.org/10.1177/1687814016651557.

Lin, L., Mao, Q., Xia, Y., Zhu, Z., Yang, D., Guo, B., Lan, H., 2017. Experimental study of specific matching characteristics of tunnel boring machine cutter ring properties and rock. Wear 378–379, 1–10. https://doi.org/10.1016/j.wear.2017.01.072.

Liu, Q., Liu, J., Pan, Y., Zhang, X., Peng, X., Gong, Q., Du, L., 2017. A wear rule and cutter life prediction model of a 20-in. TBM cutter for granite: a case study of a water conveyance tunnel in China. Rock Mech. Rock Eng. 50, 1303–1320. https://doi.org/10.1007/s00603-017-1176-4.

Ma, H., Gong, Q., Wang, J., Yin, L., Zhao, X., 2016. Study on the influence of confining stress on TBM performance in granite rock by linear cutting test. Tunn. Undergr. Space Technol. 57, 145–150. https://doi.org/10.1016/j.tust.2016.02.020.

Macias, F.J., Dahl, F., Bruland, A., 2016. New rock abrasivity test method for tool life assessments on hard rock tunnel boring: the rolling indentation abrasion test (RIAT). Rock Mech. Rock Eng. 49, 1679–1693. https://doi.org/10.1007/s00603-015-0854-3.

Mohtarami, E., Baghbanan, A., Hashemolhosseini, H., 2017. Prediction of fracture trajectory in anisotropic rocks using modified maximum tangential stress criterion. Comput. Geotech. 92, 108–120. https://doi.org/10.1016/j.compgeo.2017.07.025.

Mohtarami, E., Baghbanan, A., Hashemolhosseini, H., Bordas, S.P.A., 2019. Fracture mechanism simulation of inhomogeneous anisotropic rocks by extended finite element method. Theor. Appl. Fract. Mech. 104, 102359. https://doi.org/10.1016/j.tafmec.2019.102359.

Mohtarami, E., Baghbanan, A., Hekmatnejad, A., Rinne, M., 2022. Experimental and numerical study of fracturing in degraded and graded crystalline rocks at the laboratory scale. Int. J. Rock Mech. Min. Sci. 160, 105255. https://doi.org/10.1016/j.ijrmms.2022.105255.

Moon, T., Oh, J., 2012. A study of optimal rock-cutting conditions for hard rock TBM using the discrete element method. Rock Mech. Rock Eng. 45, 837–849. https://doi.org/10.1007/s00603-011-0180-3.

Norouzi, S., Baghbanan, A., Khani, A., 2013. Investigation of grain size effects on Micro/Macro-mechanical properties of intact rock using voronoi element—discrete element method approach. Part. Sci. Technol. 31, 507–514. https://doi.org/10.1080/02726351.2013.782929.

Oggeri, C., Oreste, P., 2012. The wear of tunnel boring machine excavation tools in rock. Am. J. Appl. Sci. 9, 1606–1617. https://doi.org/10.3844/ajassp.2012.1606.1617.

Ramalho, A., Miranda, J.C., 2006. The relationship between wear and dissipated energy in sliding systems. Wear 260, 361–367. https://doi.org/10.1016/j.wear.2005.02.121.

Richard, T., Detournay, E., Drescher, A., Nicodeme, P., Fourmaintraux, D., 1998. The scratch test as A means to measure strength of sedimentary rocks. SPE/ISRM Rock Mechanics in Petroleum Engineering. SPE-47196-MS.

Rokhy, H., Mostofi, T.M., Ozbakkaloglu, T., 2022. Calibration of different constitutive material models for Vosges sandstone due to its application in rock-cutting processes. J. Braz. Soc. Mech. Sci. Eng. 44, 468. https://doi.org/10.1007/s40430-022-03764-9.

Rostami, J., 1997. Development of a Force Estimation Model for Rock Fragmentation with Disc Cutters Through Theoretical Modeling and Physical Measurement of Crushed Zone Pressure. Colorado School of Mines, Golden, Colorado, USA, p. 249.

Rostami, J., Ozdemir, L., 1993. New model for performance production of hard rock TBMs. Proceedings - Rapid Excavation and Tunneling Conference, pp. 793–809.

Roxborough, F.F., Phillips, H.R., 1975. Rock excavation by disc cutter. Int. J. Rock Mech. Min. Sci. Geomech. Abstr. 12, 361–366. https://doi.org/10.1016/0148-9062(75)90547-1.

Schneider, E., Thuro, K., Galler, R., 2012. Forecasting penetration and wear for TBM drives in hard rock – results from the ABROCK research project/Prognose von Penetration und Verschleiß für TBM-Vortriebe im Festgestein – erkenntnisse aus dem Forschungsprojekt ABROCK. Geomech. Tunn. 5, 537–546. https://doi.org/10.1002/geot.201200040.

Shang, X., Zhou, J., Liao, X., Liu, F., Shen, J., 2024. Peridynamics simulation of TBM cutting process in soft and hard composite strata with a simplified loading scheme. Comput. Geotech. 171, 106387. https://doi.org/10.1016/j.compgeo.2024.106387.

Shang, X., Zhou, J., Liu, F., Jiang, Y., Liao, X., 2025. Three-dimensional peridynamics modeling of rock cutting considering disc cutter rolling motion. Acta Geotechnica 20, 1643–1660. https://doi.org/10.1007/s11440-025-02595-x.

Shang, X., Zhou, J., Liu, F., Shen, J., Liao, X., 2023. A peridynamics study for the free-surface-assisted rock fragmentation caused by TBM disc cutters. Comput. Geotech. 158, 105380. https://doi.org/10.1016/j.compgeo.2023.105380.

She, L., Hu, C-c, Li, Y-l, Zhang, S-r, Wang, C., Wang, Y-j, He, M-m, Li, S-m, Wang, S-l, 2024. An empirical method for estimating TBM penetration rate using tunnelling specific energy. Tunn. Undergr. Space Technol. 144, 105525. https://doi.org/10.1016/j.tust.2023.105525.

Su, P.C., Wang, W.S., Huo, J.Z., Li, Z., 2010. Optimal layout design of cutters on tunnel boring machine. J. NEU (Nat. Sci.) 31, 877–881.

Sun, J., Wang, K., Wei, J., Shang, Y., Sun, C., Ma, F., 2023. A mechanics model of constant cross-section type disc cutter based on dense core forming mechanism. Tunn. Undergr. Space Technol. 140, 105301. https://doi.org/10.1016/j.tust.2023.105301.

Sun, Z., Zhao, H., Hong, K., Chen, K., Zhou, J., Li, F., Zhang, B., Song, F., Yang, Y., He, R., 2019. A practical TBM cutter wear prediction model for disc cutter life and rock wear ability. Tunn. Undergr. Space Technol. 85, 92–99. https://doi.org/10.1016/j.tust.2018.12.010.

Thyagarajan, M.V., Rostami, J., 2024. Study of cutting forces acting on a disc cutter and impact of variable penetration measured by full scale linear cutting tests. Int. J. Rock Mech. Min. Sci. 175, 105675. https://doi.org/10.1016/j.ijrmms.2024.105675.

Wan, Z., Sha, M., Zhou, Y., 2002. Study on disc cutters for hard rock (1)—application of TB880E TBM in Qinling tunnel. Mod. Tunn. Technol. 39, 1–11. https://doi.org/10.13807/j.cnki.mtt.2002.05.001.

Wang, L., Kang, Y., Cai, Z., Zhang, Q., Zhao, Y., Zhao, H., Su, P., 2012. The energy method to predict disc cutter wear extent for hard rock TBMs. Tunn. Undergr. Space Technol. 28, 183–191. https://doi.org/10.1016/j.tust.2011.11.001.

Wang, R., Wang, Y., Li, J., Jing, L., Zhao, G., Nie, L., 2020. A TBM cutter life prediction method based on rock mass classification. KSCE J. Civ. Eng. 24, 2794–2807. https://doi.org/10.1007/s12205-020-1511-2.

Xiao, N., Zhou, X.-P., Gong, Q.-M., 2017. The modelling of rock breakage process by TBM rolling cutters using 3D FEM-SPH coupled method. Tunn. Undergr. Space Technol. 61, 90–103. https://doi.org/10.1016/j.tust.2016.10.004.

Yang, H., Liu, B., Wang, Y., Li, C., 2021. Prediction model for normal and flat wear of disc cutters during TBM tunneling process. Int. J. GeoMech. 21, 06021002. https://doi.org/10.1061/(ASCE)GM.1943-5622.0001950.

Yang, H., Wang, H., Zhou, X., 2016. Analysis on the rock–cutter interaction mechanism during the TBM tunneling process. Rock Mech. Rock Eng. 49, 1073–1090. https://doi.org/10.1007/s00603-015-0796-9.

Zahiri, M., Goshtasbi, K., Khademi Hamidi, J., Ahangari, K., 2020. A numerical investigation of TBM disc cutter life prediction in hard rocks. J. Min. Environ. 11, 1095–1113. https://doi.org/10.22044/jme.2020.9933.1922.

Zhang, Z., Aqeel, M., Li, C., Sun, F., 2019. Theoretical prediction of wear of disc cutters in tunnel boring machine and its application. J. Rock Mech. Geotech. Eng. 11, 111–120. https://doi.org/10.1016/j.jrmge.2018.05.006.

Zhao, X.B., Yao, X.H., Gong, Q.M., Ma, H.S., Li, X.Z., 2015. Comparison study on rock crack pattern under a single normal and inclined disc cutter by linear cutting experiments. Tunn. Undergr. Space Technol. 50, 479–489. https://doi.org/10.1016/j.tust.2015.09.002.

Zhou, X.-P., Zhai, S.-F., Bi, J., 2018. Two-dimensional numerical simulation of rock fragmentation by TBM cutting tools in mixed-face ground. Int. J. GeoMech. 18, 06018004. https://doi.org/10.1061/(ASCE)GM.1943-5622.0001081.